

Microstructural evolution of TiC/a-C nanocomposite coatings with pulsed magnetron sputtering

Y. T. Pei¹, K. P. Shaha¹, C. Q. Chen¹, J. Th. M. De Hosson¹,
J. W. Bradley², S. Voronin² & M. Cada²

¹*Department of Applied Physics, The Netherlands Institute for Metals Research, University of Groningen, Groningen, The Netherlands*

²*Department of Electrical Engineering and Electronics, University of Liverpool, Liverpool, UK*

Abstract

The microstructure and property of magnetron sputtered coatings are strongly affected by the intensity of concurrent ion impingement, in particular, by the energy distribution of impinging ions and the flux ratio between impinging ions and depositing atoms. In this paper, we report some striking results in the microstructure manipulation and residual stress control of TiC/a-C nanocomposite coatings with pulsed-DC magnetron sputtering. Ion mass/energy spectrometry of plasma diagnostics reveals that, depending on the waveform, frequency and width of pulses, pulsing the magnetrons can control the flux and energy distribution of Ar⁺ ions over a very broad range, in comparison with DC sputtering. The latter delivers only low energy Ar⁺ ions and also less flux. With increasing pulse frequency, the nanocomposite coatings exhibit evolutions in the morphology of growing interface from rough to smooth and in the microstructure from strongly columnar to non-columnar. AFM, SEM, HR-TEM and nanoindentation are employed to characterize the deposited coatings, supported with plasma diagnostic experiments for a better understanding of the pulsed sputtering process.

Keywords: pulsed magnetron sputtering, ion energy distribution, plasma diagnostics, microstructural evolution, nanocomposite coating.



1 Introduction

Pulsed DC magnetron sputtering in combination with the unbalanced magnetron configuration has become a major technique in the deposition of advanced coatings during the last decade [1, 2, 3]. It has the significant advantage over DC magnetron sputtering in suppressing the formation of arcs on the cathodes/targets. In particular it improves the microstructure and properties of dielectric films, which strongly depend on the intensity of the concurrent ion impingement on the growing interface of a deposited film. The crucial parameters determining the intensity of ion impingement are the energy distribution of the impinging ions and the flux ratio between impinging ions and depositing atoms. It has been observed that pulsing magnetrons in mid frequency (up to 350 kHz) leads to a much extended energy distribution of impinging ions and rather high ion current density towards the substrate [4, 5]. As a result, dense and well-structured dielectric and metallic coatings can be grown in pulsed mode [6]. However, a thorough understanding of the mechanism of plasma controlling and microstructure manipulation with pulsed DC sputtering is still lacking.

Our recent work shows that the column boundaries (CBs) of TiC/a-C:H nanocomposite coatings are a potential source of failure under loading and contact sliding [7, 8]. The CBs are harmful as initiation site of cracks and preferential cracking path, attributed to the fact that the homogeneity of nanocomposite is interrupted by the CBs that are enriched in carbon and voids. In reactive sputtering, the CBs can be readily restrained by employing a high voltage substrate bias or increasing the carbon content in the coatings. The mechanism of column restraint in this case results in a smooth growing interface of deposited coatings via intensive ion impingement and highly mobile carbon adatoms. However, it is hardly applicable to DC non-reactive sputtering of TiC/a-C nanocomposite coatings, where the landing of sputtered atoms interrupts and ion impingement may fluctuate to a large extent when the substrates pass from one target to another. The purpose of this work is to study the effects of pulsed DC sputtering on the depositing process and microstructure evolution of TiC/a-C nanocomposite coating, in particular, on the restraint of column growth. The results are striking in the sense of microstructure optimization and plasma manipulation.

2 Experiments

TiC/a-C nanocomposite coatings were deposited with non-reactive sputtering in a TEER UDP400/4 closed-field unbalanced magnetron sputtering (CFUMS) system. The system was configured of one Ti target (99.7%), one Cr target (99.95%) and two graphite targets (99.999%) opposite to each other. The two magnetrons with a metallic target were powered by a Pinnacle 6/6 kW double channel DC power supply (Advanced Energy) and the other two magnetrons with graphite targets were powered by a Pinnacle Plus 5/5 kW double channel pulsed DC power supply (Advanced Energy). The substrates were biased by a Pinnacle Plus 5 kW single channel pulsed DC power supply (Advanced Energy). All the power supplies for sputtering were operated at current control mode via a



computer controlling system. The UDP 400/4 system was installed with an oil-free pumping system (a turbo molecular pump plus a diaphragm backing pump). The base pressure before deposition was $3\sim 4 \times 10^{-6}$ mbar and the deposition pressure 2.6×10^{-3} mbar controlled by a constant flow rate of argon gas. No intended heating on the substrates was used during deposition.

The substrates used for each coating were $\phi 30 \times 6$ mm discs of hardened M2 steel for tribological tests and $\phi 100$ mm Si wafer for microscopic observation of coating fracture cross-sections and for residual stress measurements by monitoring the curvature change. A 200 nm thick ductile CrTi interlayer of optimized composition and structure was employed to enhance the interfacial adhesion of TiC/a-C nanocomposite coatings. The interfacial adhesion was quantified by scratch tests with a CSM Revetester. The hardness and indentation modulus of the coatings were measured by nanoindentation with an MTS Nanoindenter XP[®]. The microstructural evolutions of the coatings were characterized with high resolution scanning electron microscopy (HR-SEM) on fracture cross sections and atomic force microscopy was used to image the surface morphology and to measure the surface roughness. The nanostructure of the coatings was revealed with high resolution transmission electron microscopy.

An EQP300 quadrupole mass spectrometer/ion energy analyser (Hiden Analytical Ltd) was used to measure the energy distribution of impinging ions in a single unbalanced magnetron sputtering system, GENLAB (GENCOA Ltd), installed with a $\phi 150$ mm circular magnetron. It had a typical unbalanced configuration of adjustable magnetic field strength, which was set to resemble the field strength of the magnetrons installed in the TEER UDP400/4 rig. The single magnetron was powered with a 5kW Pinnacle Plus unit and operated at the same sputtering parameters used for coating deposition. The extractor head of the EQP300 instrument was pointed to the racetrack of the target and fixed directly behind a metallic substrate, which had a large opening hole that was covered with a fine nickel grid and aligned with the entrance orifice ($\phi 300 \mu\text{m}$) of the extractor. For the detailed setup see [4]. The ion energies were effectively measured with reference to ground potential and averaged during a measure time of one second. Therefore, the ion counts of different energies were a direct measure of the ion flux and can be confidently compared between measurements, provided the instrument settings remained unchanged.

3 Results and discussions

3.1 DC magnetron sputtering of TiC/a-C nanocomposite coatings

In our recent work on the deposition of TiC/a-C:H nanocomposite coatings with reactive DC sputtering in an argon/acetylene atmosphere, it has been revealed that the undesired columnar microstructure can be fully restrained by applying a higher substrate bias voltage (up to 150V) or/and a higher flow rate of acetylene gas that corresponds to a maximum carbon content of 88 at.% (excluding hydrogen) [7]. The columnar growth is directly related to the interface structure of the growing coatings. Typical cauliflower-like patterns characterize the surface topography of the nanocomposite coatings such that the cauliflower



branches are separated by groove networks with a maximum depth of about 10 nm. These deep groove networks are likely the origin of the columnar boundaries (CBs), which is supported by the fact that the CBs intersect with the growing interfaces at the deep groove networks [9]. One can imagine that restraining the formation of groove networks will lead to the destruction of CBs and thus a column-free coating. In fact, the mechanisms involved in manipulating the two deposition parameters (bias voltage and flow rate of acetylene) are different. That is to say, the former breaks down the groove structure through intensive ion impingement and the latter directly fills the grooves with hydrocarbon adatoms of high mobility, respectively.

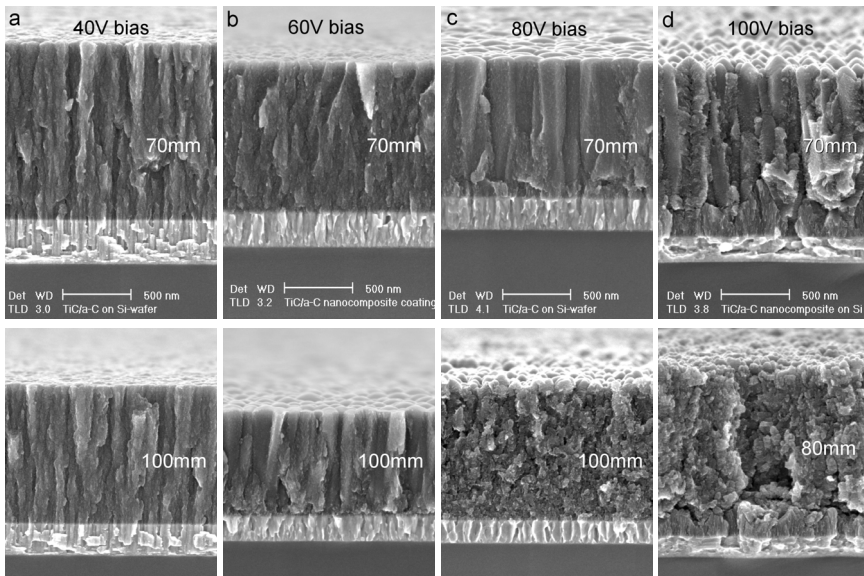


Figure 1: SEM micrographs showing the fracture cross sections of TiC/a-C nano-composite coatings deposited with DC sputtering at different substrate bias voltage (two hours deposition time): (a) 40V, (b) 60V, (c) 80V and (d) 100V with indicated distance from the targets.

Following this approach, hydrogen-free TiC/a-C nanocomposite coatings have been deposited by non-reactive magnetron sputtering graphite and titanium targets. Figure 1 shows the microstructural evolution of DC sputtered TiC/a-C coatings of nearly the same composition with increasing substrate bias voltage. It is obvious that the columnar microstructure is always present in the coatings, even though the columns become thicker and the coatings get denser with increasing the bias voltage up to 80V. Further increase of the bias voltage to 100V makes the columnar character stronger and the coating looser in reverse, due to the formation of facets on the head of growing columns and thus a much rougher interface of the growing coating. Finally, the coating deposited at 120V bias voltage flakes off. There is no way to fully suppress the columnar

microstructure of TiC/a-C nanocomposite coatings by only increasing substrate bias voltage under DC magnetron non-reactive sputtering. In addition, it is worth to note that an increase in substrate bias voltage narrows the space suitable for depositing the coatings, in terms of the distance from targets. When applying a lower negative bias voltage (40 V or 60 V), it is possible to deposit dense coatings at the distance of 100 mm from the targets though the deposition rate is lower than that at the distance of 70 mm (Figs. 1(a) and 1(b)). However, the coating deposited at the same distance of 100 mm becomes porous and very loose once the bias voltage is increased to 80 V. An even worse situation is at 100V bias where the coating deposited at 80 mm distance is already porous (Fig. 1(d)). In this case, only the coating deposited at 60 mm distance from the targets is fully dense but still with a columnar microstructure (not shown). Such a reduction of suitable space for deposition is attributed to the over impingement of highly energetic but low flux ions, as to be discussed in the next session.

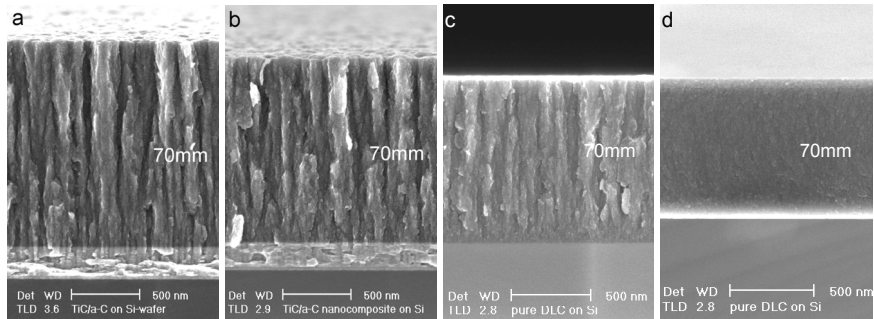


Figure 2: SEM micrographs showing the fracture cross sections of TiC/a-C nano-composite coatings deposited with DC sputtering at 60V substrate bias and of different carbon content: (a) 82 at.%, (b) 94 at.%, (c) 100 at.% and (d) 100 at.% on a stationary substrate.

The next step in our study of DC sputtering deposition parameters is to vary the carbon content of the coatings and to check the effect on the restraint of columnar growth. The results are shown in Fig. 2. By increasing the carbon content from 82 at.% to 94 at.%, the columnar character of the coatings does not show an essential difference, except for the fact that the coating of higher carbon content becomes slightly denser. Even the coating of pure carbon exhibits columnar microstructure (Fig. 2(c)). Apparently, the effect of increasing carbon content is minor in restraining the columnar growth, which is rather different from the situation of reactively sputtered TiC/a-C:H nanocomposite coatings [7]. In conclusion, it is almost impossible to deposit column-free TiC/a-C coatings with DC magnetron sputtering. The only exception is the pure carbon coating deposited on the substrate that is kept stationary in front of the graphite target (Fig. 2(d)), where a continuous impingement of high flux ions is available. In this sense, it provides a clue how to prohibit the columnar microstructure in TiC/a-C coatings. That is to enhance the flux of the impinging ions especially during the travel of substrates passing from one target to another.

3.2 Pulsed-DC magnetron sputtering of TiC/a-C nanocomposite coatings

Figure 3 shows the fracture cross section of the TiC/a-C coatings deposited with pulsed DC magnetron sputtering. Switching from DC to pulsed DC (*p*-DC) sputtering of 100 kHz frequency, the columnar microstructure does not change much, but becomes more diffuse CBs (Fig. 3(a)). By increasing the frequency of sputtering DC pulses to 250 kHz and keeping all the other parameters unchanged, the coating surface becomes much smoother and the columnar feature is almost invisible. Up to 350 kHz pulsed DC sputtering, the deposited coating is fully columnar free, with a surface (actually the growing interface) so smooth that it hardly shows some contrast under the magnification used for SEM observation. It should be pointed out that the restraint of columnar microstructure with pulsed DC sputtering is achieved at the expense of a reduced deposition rate. The deposition rate of TiC/a-C coatings at 50% duty cycle and *p*-DC frequency 100 kHz, 250 kHz and 350 kHz is 80%, 60% and 58%, respectively, of the deposition rate with DC sputtering. Obviously, the reduction extent of deposition rate is dependent on the sputtering yield of different kinds of targets at different frequencies and the duty factor. Once the *p*-DC frequency is above 250 kHz, the deposition rate does not significantly decrease any further.

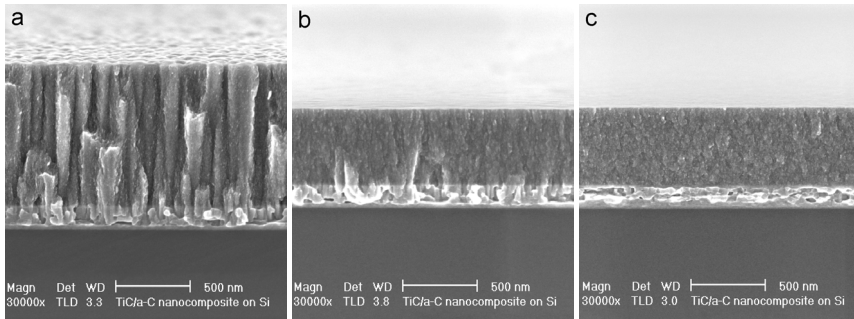


Figure 3: SEM micrographs showing the fracture cross sections of TiC/a-C nano-composite coatings deposited with pulsed-DC sputtering at 40V substrate bias and different pulse frequency (50% duty cycle): (a) 100 kHz, (b) 250 kHz and (c) 350 kHz (deposition time: two hours).

It is interesting to note that, under *p*-DC sputtering, the space suitable for coating deposition is wide enough. As shown in Fig. 4(a), the thickness of the coatings changes inversely as a function of the distance from the targets but its negative slope is smaller than that with DC sputtering. Moreover, the coatings deposited in the distance range of 60-100 mm exhibit continuously a dense and columnar free microstructure. This feature is of particular importance for industrial applications where workpieces of large sizes or large quantity of workpieces need to be coated in one batch. The optimized microstructure of TiC/a-C coating deposited with *p*-DC magnetron sputtering is shown in Fig.

4(b), consisting of a ductile interlayer, smooth and mirror-like surface, and fine and column-free microstructure.

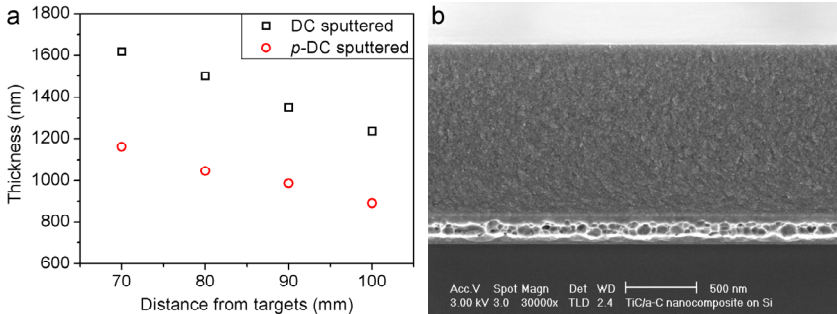


Figure 4: (a) Thickness of deposited coatings versus the distance from the targets and (b) optimized microstructure of TiC/a-C nanocomposite coatings.

3.3 Ion energy distribution and plasma diagnostics of *p*-DC sputtering

To understand the mechanism of column restraint under *p*-DC magnetron sputtering, ion mass/energy spectrometry has been employed to diagnose the sputtering plasma, in particular the energy distribution and flux of the impinging Ar^+ ions pulled onto the growing interface of the coatings. Figure 5 presents the *p*-DC voltage waveform applied onto the targets, time resolved energy distribution and the flux of the impinging Ar^+ ions. The voltage waveform of the asymmetric bipolar pulsed DC exhibits three characteristic periods: the pulse on period A, the reversing period B and the pulse off period C. The significant features of the asymmetric bipolar *p*-DC power supplies used in this research include the overshoot peak of around 200 V and the adjacent fluctuations in the reversing period B as well as the low positive voltage remaining during the pulse off period C. The time averaged energy distribution curves of the impinging Ar^+ ions under *p*-DC magnetron sputtering present three distinct populations of the ions that reflect the target voltage waveforms. That is to say, impingements of Ar^+ ions of low energy (< 20 eV, peak A in Fig. 5(b)) occur during the pulse-on period, supported by the fact that DC magnetron sputtering produces only the low energy ions of the same category. The ions of intermediate energy (20~50 eV, peak C in Fig. 5(b)) are generated during the pulse-off period, which is evident because the population of this category ions diminishes with decreasing pulse-off period (i.e. increasing the duty cycle at a chosen *p*-DC frequency) as shown in Fig. 5(c). Those ions of high energy extending over 200 eV are created during the reversing period. Because of the detection limit of the energy spectrometer, the energy distribution function curves at a *p*-DC frequency above 200 kHz are partly cut off beyond 195 eV. It is clear that the energy distribution function of the impinging Ar^+ ions is governed by the sputtering mode, *p*-DC frequency and the duty cycle.

More important in control of the microstructure of the coatings is the flux of the impinging ions generated in the sputtering plasma. As shown in Fig. 5(d), the flux of the total impinging Ar^+ ions at p -DC sputtering mode of low frequencies (e.g. 100 kHz) is comparable with that under DC magnetron sputtering. However, the total ions flux dramatically increases with increasing the frequency beyond 100 kHz. One should keep it in mind that the total ions flux measured at a frequency above 200 kHz is slightly lower than the true value, due to the cut off of the measurement of the high energy ions beyond 195 eV. This explains the smaller increase of the measured ion flux between the high frequencies (Fig. 5(d)). It is clear that the flux of total impinging ions may differ by one order of magnitude between DC magnetron sputtering and p -DC magnetron sputtering at high frequencies. In particular, the impinging ions in the intermediate and high energy bands become more and more dominant with increasing p -DC frequency, delivering much more energy for impingement on the growing interface of deposited coatings.

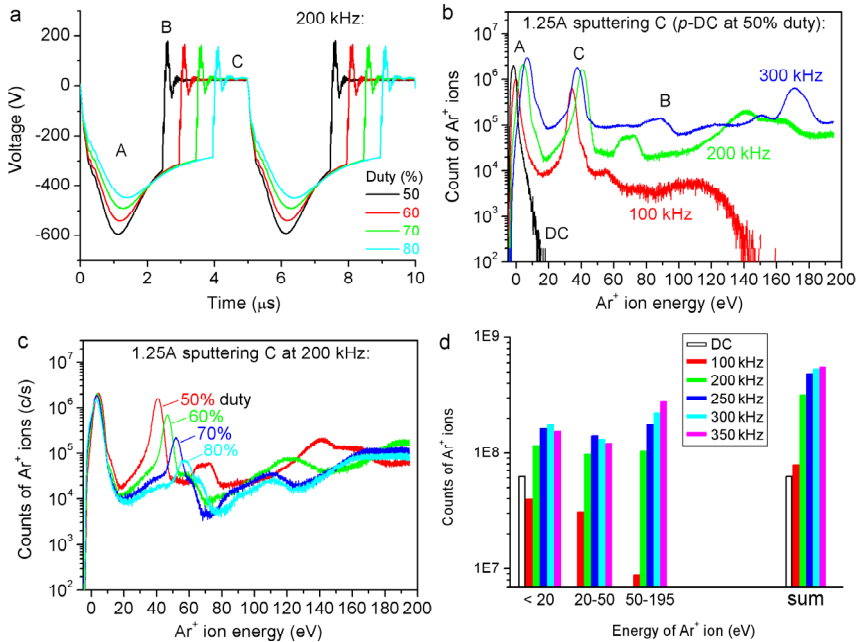


Figure 5: (a) Voltage waveform of p -DC at 200 kHz; energy distribution of impinging Ar^+ ions incident on the growing coatings under DC sputtering or pulsed DC sputtering of different frequencies (b) and different duty cycles at 200 kHz (c); (d) flux of the Ar^+ ions in three energy ranges as well as the sum at different p -DC frequencies.

Besides the enhancement on the flux and energy distribution of impinging ions, another significant feature of p -DC magnetron sputtering is the expansion of the plasma torch in between the unbalanced magnetrons. Figure 6 compares

the confine of the plasma torch incident onto the substrate at different sputtering modes and frequencies. Under DC sputtering, the dense plasma torch confined in front of the target can cover only the center part of the substrate (Fig. 6(a)). In contrast, the plasma torch at 100 kHz *p*-DC sputtering covers nearly the whole substrate, but with a large intensity difference from the center to the outer fringe (Fig. 6(b)). Up to 250 kHz, the plasma torch gets much denser and homogeneously covers the entire substrate (Fig. 6(c)). It even expands to the surrounding area but the intensity is still very low. At the highest frequency 350 kHz, the extensive plasma not only covers the entire substrate but also fills in the whole chamber (Fig. 6(d)). It is this expanded plasma that keeps the growing coating under intensive and in particular continuous impingement when passing by from one target to another in a closed-field configuration of multi-targets sputtering system.

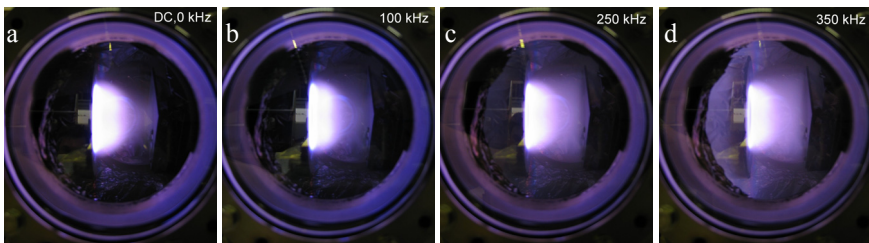


Figure 6: Photos showing the shape and density of the plasma incident at the rectangular substrate positioned to the right of viewport. A much denser and extended plasma is obtained at higher frequency pulsed DC sputtering, compared with DC sputtering.

In the so called closed-filed unbalanced magnetron sputtering system such as the Teer UDP 400/4 rig used in this work, targets stand vertically along the circular chamber wall and the substrates mounted on the sample carousel rotate around the central axis of the chamber (single spindle rotation) and pass at a chosen distance the targets one by one. For reactive sputtering, the decomposition of the reactive gases occurs in the plasma everywhere inside the chamber and provides some of the species for deposition that continuously reach the growing film from various angles and at any position, besides the sputtered atoms from the targets. Even in non-reactive sputtering with a co-planar configuration of magnetrons facing towards the same area or a substrate, such a continuous landing of different kinds of depositing atoms can be readily realized as well. Therefore, there is less challenge in control of the microstructure of DLC based composite coatings in these two cases. Different from the preceding situation, during non-reactive sputtering with a closed-filed unbalanced magnetron sputtering system the landing of sputtered atoms interrupts and ion impingement may fluctuate to a large extent in between the targets. This may readily lead to either multilayered coatings due to composition variation or undesired microstructures because of unstable ion impingement. This work focuses on the influence of pulsed magnetron sputtering on the depositing

process and consequently the microstructure evolution of the deposited coatings, rather than the sputtering process itself. It is clearly demonstrated that pulsing the unbalanced magnetrons may dramatically change the property of the plasma and consequently enhance the intensity of the concurrent ion impingement on the growing interface of deposited coating, in comparison with DC sputtering. As a result, a desired microstructure may be readily tailored to achieve the superior performances of advanced coatings.

4 Conclusions

Pulsed DC magnetron sputtering can control the flux and energy distribution of Ar^+ impinging ions over a very broad range, in comparison with DC sputtering that delivers only low energy Ar^+ ions and also much smaller flux. The most striking result observed is the capability in the microstructure manipulation of TiC/a-C nanocomposite coatings with pulsed-DC magnetron sputtering, especially constraining the formation of columnar microstructure. With increasing the pulse frequency, the nanocomposite coatings exhibit evolutions in morphology of the growing interface from rough to smooth, in the microstructure from strongly columnar to non-columnar and become fully dense.

Acknowledgements

The authors acknowledge financial support from the Netherlands Institute for Metals Research (NIMR) and the Foundation for Fundamental Research on Matter (FOM-Utrecht).

References

- [1] S. Schiller, K. Goedicke, J. Reschke, V. Kirchhoff, S. Schneider and F. Milde. *Surf. Coat. Technol.*, 61 (1993), 331-337.
- [2] P.J. Kelly and R.D. Arnell. *Vacuum*, 56 (2000), 159-172.
- [3] R.D. Arnell, P.J. Kelly and J.W. Bradley. *Surf. Coat. Technol.*, 188 (2004), 158-163.
- [4] J.W. Bradley, H. Bäcker, Y. Aranda-Gonzalvo, P.J. Kelly and R.D. Arnell. *Plasma Source Sci Technol.*, 11 (2002), 165-174.
- [5] H. Bartzsch, P. Frach and K. Goedicke. *Surf. Coat. Technol.*, 132 (2000), 244-250
- [6] P.J. Kelly and R.D. Arnell. *J. Vac. Sci. Technol.* A17 (1999), 945-953
- [7] Y.T. Pei, D. Galvan and J.Th.M. De Hosson. *Acta Mater.*, 53 (2005), 4505-4521.
- [8] D. Galvan, Y.T. Pei and J.Th.M. De Hosson. *Surf. Coat. Technol.*, 200 (2006), 6718-6726.
- [9] J.Th.M. De Hosson, Y.T. Pei and D. Galvan. *Surfaces and Interfaces in Nanostructured Materials II*. Eds: *S.M. Mukhopadhyay, N.B. Dahotre, S. Seal, and A. Agarwal*. TMS, 2006. 59-68.

